



23 remains challenging, due to spatiotemporally heterogeneous responses of wildfires to
24 climate variability and human influences. Here, we developed an interpretable Machine
25 Learning (ML) fire model (AttentionFire_v1.0) to resolve the complex spatial-
26 heterogeneous and time-lagged controls from climate on burned area and to better
27 predict burned areas over ASA regions. Our ML fire model substantially improved
28 predictability of burned area for both spatial and temporal dynamics compared with
29 five commonly used machine learning models. More importantly, the model revealed
30 strong time-lagged control from climate wetness on the burned areas. The model also
31 predicted that under a high emission future climate scenario, the recently observed
32 declines in burned area will reverse in South America in the near future due to climate
33 changes. Our study provides reliable and interpretable fire model and highlights the
34 importance of lagged wildfire-climate relationships in historical and future predictions.

35

36 1. Introduction

37 Wildfires modify land surface characteristics, such as vegetation composition, soil
38 carbon, surface runoff, and albedo, with significant consequences for regional carbon,
39 water, and energy cycles [Benavides-Solorio and MacDonald, 2001; Randerson *et al.*,
40 2006; Shvetsov *et al.*, 2019]. Over African and South American (ASA) regions, where
41 more than 70% of global burned area occurs, wildfires emit $\sim 1.4 \text{ PgC yr}^{-1}$ and dust and
42 aerosols that can alter regional climate through radiative processes [Etminan *et al.*, 2016;
43 Ramanathan *et al.*, 2001; Werf *et al.*, 2017]. While greenhouse gas emissions contribute
44 to climate change, other toxic species and airborne particulate matter from wildfires



45 lead to substantial health hazards, including elevated premature mortality [*Knorr et al.*,
46 2017; *Lelieveld et al.*, 2015]. In particular, wildfire particulate matter emissions across
47 tropical regions have exceeded current anthropogenic sources and are predicted to
48 dominate future regional emissions [*Knorr et al.*, 2017].

49 Although total tropical wildfire burned area has declined over the past few decades
50 due to climate change and human activities [*Andela et al.*, 2017; *Andela and Van Der*
51 *Werf*, 2014] (e.g., from increases in population density, cropland fraction, and livestock
52 density), wildfire still plays a significant role in mediating surface climate [*Xu et al.*,
53 2020], biogeochemical cycles, and human health [*Andela et al.*, 2017]. Further, 21st
54 century projections of increases in temperature, regional drought [*Dai*, 2013; *Taufik et*
55 *al.*, 2017], and precipitation variations may outweigh these direct human impacts and
56 result in unprecedentedly fire-prone environments over a large fraction of Africa
57 [*Andela and Van Der Werf*, 2014; *Archibald et al.*, 2009; *Van Der Werf et al.*, 2008] and
58 South America [*Malhi et al.*, 2008; *Pechony and Shindell*, 2010]. These factors
59 highlight the need for better understand, predict, and management of these critical fire
60 regions to minimize economic losses, human health hazards, and natural ecosystem
61 degradation. Therefore, improved understanding and accurate prediction of wildfire
62 activity is increasingly important for effective fire management and sustainable
63 decision-making.

64 Climate is acknowledged one of the most dominant controllers on ASA wildfires
65 [*Andela et al.*, 2017; *Chen et al.*, 2011]. For example, precipitation variations contribute
66 substantially to burned area patterns in southern and northern Africa [*Andela and Van*



67 *Der Werf*, 2014; *Archibald et al.*, 2009], and are also closely linked to wildfire
68 spatiotemporal dynamics in south America [*Chen et al.*, 2011; *Malhi et al.*, 2008; *Van*
69 *Der Werf et al.*, 2008]. More importantly, the strong controls from climate on wildfires
70 often show time-lags and the time-delay can be up to multiple months [*Andela and Van*
71 *Der Werf*, 2014; *Van Der Werf et al.*, 2008], which enables wildfire predictions ahead
72 of fire season [*Chen et al.*, 2016; *Chen et al.*, 2020; *Chen et al.*, 2011; *Turco et al.*,
73 2018]. The spatiotemporal responses of wildfires to climate changes are complicated
74 by non-linear interactions among climate, vegetation, and human activities [*Andela et*
75 *al.*, 2017; *Van Der Werf et al.*, 2008]. In more xeric subtropical regions, increasing
76 precipitation during the wet season can be the dominant controller on increasing
77 wildfire during the following dry season (through regulation of fuel availability and
78 fuel spatial structures) [*Archibald et al.*, 2009; *Littell et al.*, 2009; *Van Der Werf et al.*,
79 2008]. In contrast, increasing precipitation in more mesic regions results in excessive
80 fuel moisture, thereby becoming the main limitation of dry-season wildfires (i.e.,
81 opposing fire trends are observed with increasing precipitation in northern and southern
82 Africa) [*Andela and Van Der Werf*, 2014; *Van Der Werf et al.*, 2008]. In addition to
83 natural processes, human activities are primary ignition sources and have shaped fire
84 patterns in the ASA regions [*Andela et al.*, 2017; *Aragao et al.*, 2008; *Archibald et al.*,
85 2009]. Fire-use types driven by local socio-economic conditions and fire management
86 policies may also affect the fire-climate relationships [*Andela et al.*, 2017]. Therefore,
87 strong climate controls from wet season to dry season need to be considered along with



88 fuel distributions and human activities for continental fire predictions under climate
89 change.

90 Accurate predictive modeling of wildfire with skillful representation of how
91 environmental and anthropogenic factors modulate the burned area is still challenging.
92 State-of-the-art process-based fire models (*e.g.*, the Fire Model Intercomparison Project
93 [*Rabin et al.*, 2017]) have reasonably simulated the spatial distribution of burned areas.
94 However, they generally do not accurately capture burned area seasonal variation and
95 inter-annual trends and variability [*Andela et al.*, 2017]. Improving predictability and
96 reducing uncertainties of process-based models require more sophisticated
97 representation of fire processes and parameterization, which remain a long-term
98 challenge [*Bowman et al.*, 2009; *Hantson et al.*, 2016; *Teckentrup et al.*, 2019]. In
99 response to this challenge, data-driven statistical or Machine Learning (ML)
100 approaches have been developed and demonstrated to effectively capture wildfire
101 severity and burned area dynamics [*Archibald et al.*, 2009; *Chen et al.*, 2020; *Chen et*
102 *al.*, 2011; *Zhou et al.*, 2020]. However, the spatially heterogenous, non-linear, and time-
103 lagged controls have been oversimplified (*e.g.*, using linear models or only considering
104 climate variables at specific time lags or seasons [*Archibald et al.*, 2009; *Chen et al.*,
105 2016; *Chen et al.*, 2020; *Chen et al.*, 2011; *Gray et al.*, 2018a]) or have been black
106 boxed, impeding an interpretable and reliable way to understand the critical
107 spatiotemporal processes from wet season to dry season [*Jain et al.*, 2020; *Reichstein*
108 *et al.*, 2019].



109 In this work, we developed a wildfire model (AttentionFire) leveraging on an
110 interpretable Long-Short-Term-Memory framework to predict wildfire burned areas
111 over Northern Hemisphere Africa (NHAF), Southern Hemisphere Africa (SHAF), and
112 Southern Hemisphere South America (SHSA) [Giglio *et al.*, 2013]. We also focused on
113 using the AttentionFire model to explore the dependency of simulated burned area on
114 different drivers from wet season to dry season across different gridcells. We assessed
115 model predictability with observed burned area from Global Fire Emission Database
116 (GFED) and compared with five other machine learning based fire models.

117

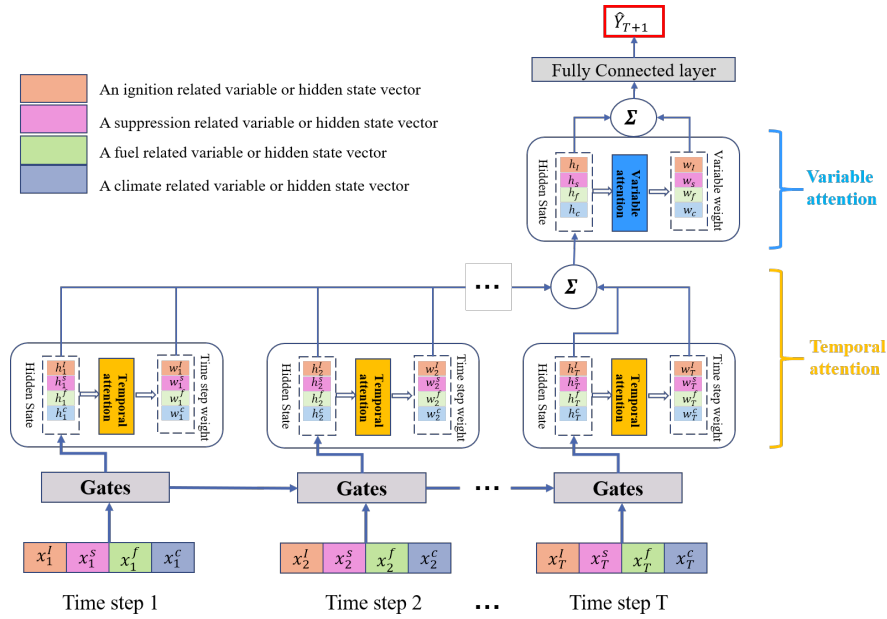
118 **2. Methods**

119 **2.1 AttentionFire model**

120 The AttentionFire model is based on an interpretable attention-augmented LSTM
121 [Guo *et al.*, 2019; Li *et al.*, 2020; Liang *et al.*, 2018; Qin *et al.*, 2017; Vaswani *et al.*,
122 2017] framework. An naïve LSTM has shown advantages in capturing short- and long-
123 term dependencies in input time series [Hochreiter and Schmidhuber, 1997]. However,
124 LSTM cannot explicitly and dynamically select important drivers from multiple driving
125 time series to make predictions [Guo *et al.*, 2019; Li *et al.*, 2020; Liang *et al.*, 2018;
126 Qin *et al.*, 2017; Vaswani *et al.*, 2017]. Further, LSTM works as a black-box, lacking
127 interpretability to identify the relative importance of each driver across different time
128 steps [Guo *et al.*, 2019; Li *et al.*, 2020; Liang *et al.*, 2018]. Attention mechanisms
129 overcome these challenges by adaptively assigning larger weights to more important
130 drivers and time steps [Liang *et al.*, 2018; Vaswani *et al.*, 2017]. Here we use attention



131 mechanism to explicitly capture controlling factors of fire predictions with various
 132 time-lags (Fig. 1). Below are detailed descriptions of the fire model.



133
 134 **Fig. 1:** An illustrative workflow for AttentionFire_v1.0 model prediction. Four kinds of
 135 drivers are considered: ignition related, suppression related, fuel, and climate. The
 136 temporal attention is used to identify important time steps for each kind of driver, while
 137 the variable attention is used to identify important drivers for final burned area
 138 prediction.

139
 140 Given four categories of time series, $X = (X^I, X^S, X^f, X^c)^T$, where T is the length
 141 of time series, we use $X^i = (x_1^i, x_2^i, \dots, x_T^i)^T \in R^T$, where $1 \leq i \leq n$, to denote the i -
 142 th time series, and use $X_t = (x_t^I, x_t^S, \dots, x_t^n)^T \in R^n$, where $1 \leq t \leq T$, to represent the
 143 vector at time step t . x_t^I, x_t^S, x_t^f , and x_t^c represent the variables of ignition (e.g.,



144 population density), suppression (e.g., road network density), fuel availability (e.g.,
 145 living biomass), and climate (e.g., precipitation) at time step t . The AttentionFire
 146 model aims to learn a nonlinear function F to map the n time series to the observed
 147 burned area Y_{T+1} at time step $T + 1$:

$$\hat{Y}_{T+1} = F(X^l, X^s, X^f, X^c)^T \quad (1)$$

148 Where \hat{Y}_{T+1} is the predicted burned area at time step $T + 1$.

149 First, the model iteratively transforms the i -th driving variable at time step t to a
 150 hidden state vector h_t^i , where $1 \leq t \leq T$ and $1 \leq i \leq n$ through LSTM gate
 151 mechanisms [Guo et al., 2019; Li et al., 2020; Liang et al., 2018; Qin et al., 2017].
 152 Second, as the importance of each time step varies, temporal attention is applied to h_t^i
 153 to calculate its corresponding weight or importance w_t^i . Third, the weighted summation
 154 h_{sum}^i of h_t^i is obtained to represent the summarized information for the i -th driving
 155 variable:

$$w_t^i = f_{attn}(h_t^i) \quad (2)$$

$$h_{sum}^i = \sum_{t=1}^T w_t^i h_t^i$$

156 Where $h_t^i \in R^m$ is the hidden state vector of the i -th driving series at time step t , that
 157 stores the summary of the past input sequence [Hochreiter and Schmidhuber, 1997].
 158 w_t^i is the calculated weight for the i -th driver at time step t through attention function
 159 f_{attn} :

$$w_t^{i'} = \tanh(W_p h_t^i) \quad (3)$$



$$w_t^i = \frac{e^{w_t^{i'}}}{\sum_{j=1}^T e^{w_t^{j'}}$$

160 where $W_p \in R^{1 \times m}$, is a parameter matrix that needs to be learned. To furtherly capture
 161 the relative importance of the i -th driving variable compared to other driving variables,
 162 variable attention is used for the summarized information h_{sum}^i and h_T^i . Note that h_T^i
 163 is also a kind of summarized information derived by the LSTM [Guo *et al.*, 2019;
 164 Hochreiter and Schmidhuber, 1997]. The weight or importance of the i -th driving
 165 variable w_i is calculated as:

$$w_i' = \tanh(W_a[h_{sum}^i, h_T^i])$$

$$w_i = \frac{e^{w_i'}}{\sum_{j=1}^n e^{w_j'}} \quad (4)$$

166 Finally, using the weighted sum of all driving variables, the model generates the
 167 prediction \hat{Y}_{T+1} :
 168

$$o_i = W_o[h_{sum}^i, h_T^i] + b_o$$

$$\hat{Y}_{T+1} = \sum_{i=1}^n o_i w_i \quad (5)$$

169 where $W_a \in R^{1 \times 2m}$, is a learnable parameter matrix and the linear function with weight
 170 $W_o \in R^m$ and bias $b_o \in R$, along with attention calculated weight w_i , produce the
 171 final prediction result. The parameters of attention-based LSTM are learned via a back-
 172 propagation algorithm by minimizing the mean-squared error between predictions and
 173 observations [Guo *et al.*, 2019; Leung and Haykin, 1991].

174 The AttentionFire model is implemented with python under Python 3 environment.
 175 The model is open-access at <https://zenodo.org/record/6903284#.YvH8F-zMJmP> under



176 Creative Commons Attribution 4.0 International license. Detailed code and descriptions
177 are included in the repository including loading datasets, model initialization, training,
178 predicting, saving parameters, and loading the trained model (see more details in code
179 availability section).

180 **2.2 Baseline models and model settings**

181 Five other widely used Machine learning (ML) models are used as baseline models
182 to compare with AttentionFire model: random forest (RF) [Coffield *et al.*, 2019; Gray
183 *et al.*, 2018b], decision tree (DT) [Amatulli *et al.*, 2006], gradient boosting decision tree
184 (GBDT) [Coffield *et al.*, 2019], artificial neuro network (ANN) [Joshi and Sukumar,
185 2021; Zhu *et al.*, 2021], and naive LSTM. The inputs of climate and fuel-related
186 variables for the first four models (non-sequence models) are variables of the latest
187 three month available for prediction [Yu *et al.*, 2020] while the corresponding inputs of
188 naive LSTM and AttentionFire models are whole-year historical time sequences which
189 cover dynamics from wet to dry seasons to capture short- and long-term dependencies
190 underlying the input sequence [Guo *et al.*, 2019; Li *et al.*, 2020; Qin *et al.*, 2017;
191 Vaswani *et al.*, 2017]. The socioeconomic predictors (i.e., population, road density,
192 livestock) consider only the more recent and available statistics typically reported at a
193 year scale. For each model, we iteratively leave one-year dataset out for testing and use
194 the remaining dataset for model training and validation. Details of the settings for used
195 models in experiments are listed in Table S1.

196 **2.3 Datasets**

197 Satellite-based global burned area dataset (Global Fire Emissions Database [Giglio *et*



198 *al.*, 2013]) is used as prediction target, and datasets of various socio-environmental
199 drivers are used as model inputs. Population density, livestock density, road-network
200 density, and land use are considered as anthropogenic factors on fire ignition and spread.
201 Fuel variables include fuel moisture, live and dead vegetation biomass. Seven
202 meteorology variables from NCEP-DOE Reanalysis are considered, including air
203 temperature, precipitation, surface pressure, wind speed, specific humidity, downward
204 shortwave radiation, and vapor pressure deficit. Details of each dataset and
205 corresponding references are listed in Table S2. The raw datasets were unified to the
206 same spatial resolution (T62 resolution: 94×192) with a covering period from 1997 to
207 2015.

208 For future projection (2016-2055) of burned area with AttentionFire model, land
209 use changes [Hurtt *et al.*, 2020], population growth, projected climate and fuel from
210 fully coupled CESM simulation under high emission scenario (ssp585) were used as
211 the ML model input. The reason to select 2016-2055 as the projected period was that
212 during 2016-2055 99th percentiles of precipitation, temperature, and vapor pressure
213 deficit were within the range of corresponding historical observations, which means
214 that the trained model has covered the range of most projected drivers in the near-future
215 and can alleviate extrapolation uncertainty caused by climate change.

216

217 **3 Results and Discussions**

218 **3.1 Model predictability on burned area spatial-temporal dynamics**

219 The AttentionFire model accurately captured the spatial distribution and temporal



variations (Fig. 2 and Fig. S1) of wildfire burned areas over NHAF, SHAF, and SHSA regions. The AttentionFire model had the lowest mean absolute errors (MAE) between model predicted and observed gridded monthly burned areas among the six ML approaches. The gridded mean absolute errors of burned area for AttentionFire were 110, 142, and 39 Kha yr⁻¹ in NHAF, SHAF, and SHSA regions, which were respectively 6%~66%, 13%~65%, and 11%~42% lower than the other 5 ML approaches in the three regions. These results highlight the capability of the AttentionFire model to capture critical driving factors of burned area across time and space.

The fact that the AttentionFire model outperformed the other five models (Fig. 2g-i) indicates the benefit of skillfully integrating time-lagged and spatially heterogeneous controls from critical drivers on wildfires. Compared to non-sequence models (i.e., RF, MLP, DT, and GBDT), the AttentionFire model adaptively captured historical dependencies of wildfires on climate conditions from wet to dry seasons [Andela and Van Der Werf, 2014; Archibald et al., 2009; Chen et al., 2011; Van Der Werf et al., 2008] (more detailed analysis is provided in next section). Compared to the naive LSTM models, the variable and temporal attention mechanisms integrated in AttentionFire has proven to be beneficial to model performance.

The spatial heterogeneity and temporal variation of wildfire responses to complex environmental and human factors have made wildfire predictions challenging, especially at large spatial scales [Andela and Van Der Werf, 2014; Chen et al., 2016; Chen et al., 2011; Littell et al., 2016; Zhou et al., 2020]. The capability of the AttentionFire model to reasonably predict spatial and temporal distributions of burned



area ahead of fire season allows more time to explore and implement management options, such as allocation of firefighting resources, fuel clearing or targeted burning restrictions [Chen *et al.*, 2011].

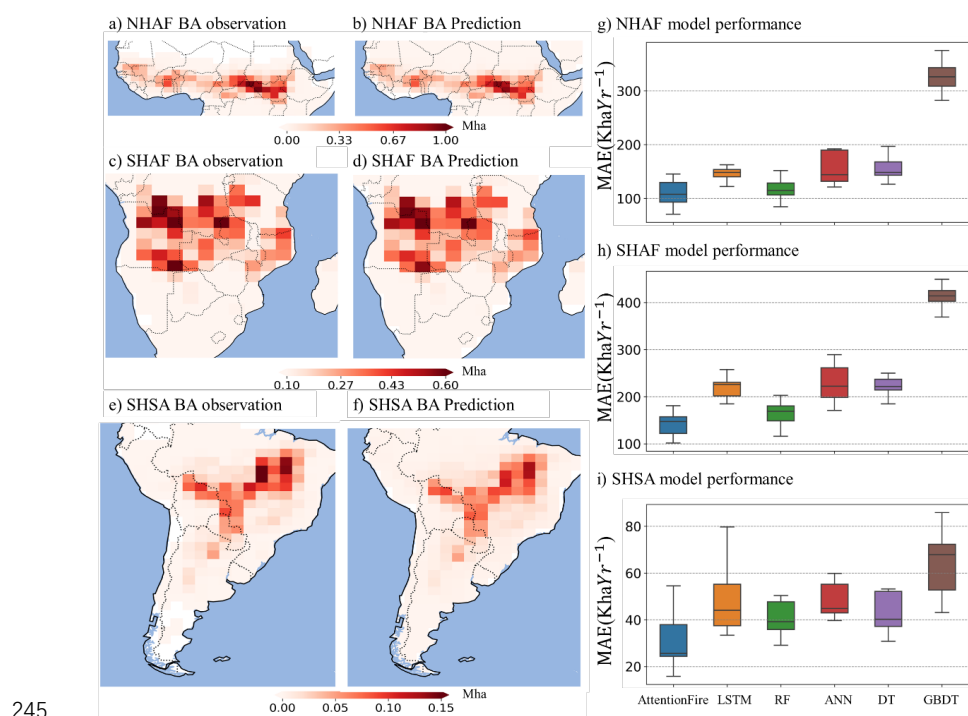
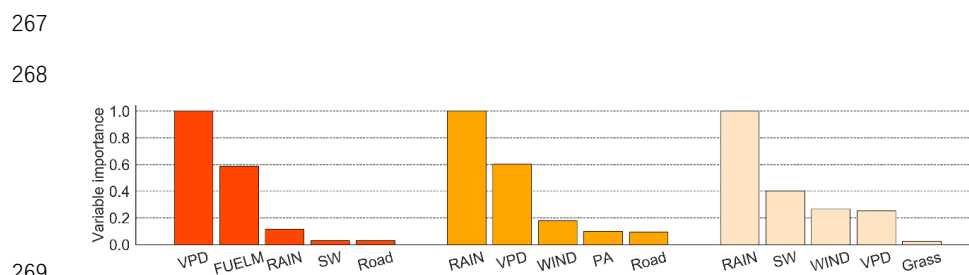


Fig. 2. The AttentionFire model accurately captured burned area spatial dynamics. (a-f) Spatial distribution of observed and AttentionFire predicted fire season mean burned areas with one-month lead time in Northern Hemisphere Africa (NHAF), Southern Hemisphere Africa (SHAF), and Southern Hemisphere South America (SHSA) regions. (g-i) Performance (in terms of mean absolute error) of AttentionFire and other five baseline models.

3.2 Dominant drivers of tropical burned area dynamics



253 The AttentionFire model dynamically weights variable importance and highlights
 254 critical temporal windows [Guo *et al.*, 2019; Li *et al.*, 2020; Liang *et al.*, 2018; Qin *et*
 255 *al.*, 2017; Vaswani *et al.*, 2017] that maximize model predictability. Therefore, the
 256 variable weights could inform dominant physical processes, while the temporal weights
 257 reflect the temporal dependency structure, making it interpretable for spatial-temporal
 258 analysis. For the AttentionFire model predictions, the variable weights showed that
 259 climate wetness exerted strong and spatial heterogenous controls on burned areas.
 260 Specifically, precipitation (for SHAF and SHSA regions) and vapor pressure deficit
 261 (VPD; for NHAF region) played the most important roles (Fig. 3) in burned area
 262 prediction during fire seasons (defined as the four months with the largest burned areas,
 263 Fig. S2), and the control strengths from those climate wetness variables on fires were
 264 significantly (one-tailed t-test, $p\text{-value} < 0.05$) stronger in regions with larger burned
 265 areas (gridcells with top 10% burned areas) than those with smaller burned areas
 266 (gridcells with last 90% burned areas) (Fig. 4 a-f).



269
 270 **Fig. 3:** Ranked top-five important variables for fire-season burned area. For each
 271 gridcell within each study region, there is a mean variable weight, representing the
 272 importance of the variable for fire prediction in the gridcell. For each region, the
 273 variable weights are summed weighted by its corresponding mean burned areas, and



274 normalized.

275

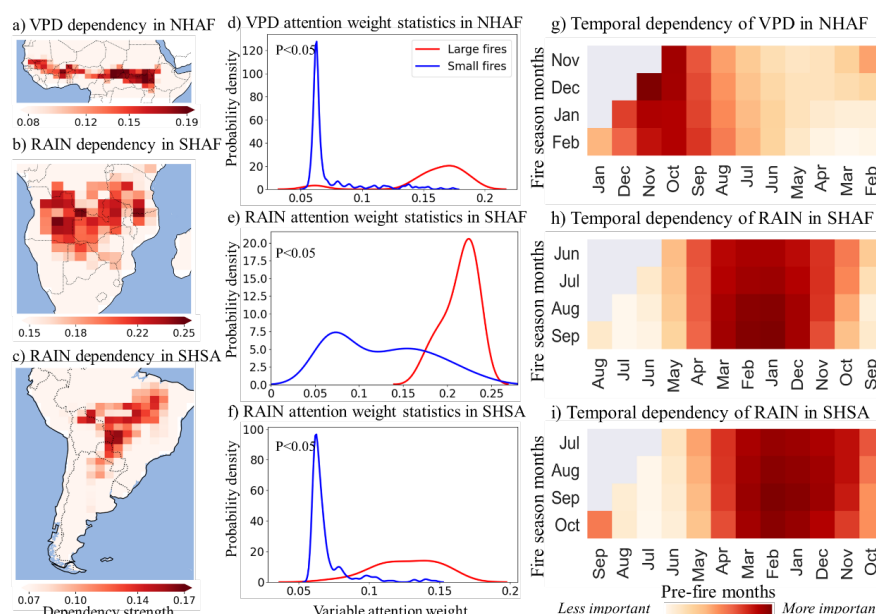
276 In AttentionFire model predictions, the precipitation and VPD explained ~66% -
277 ~80% (Fig. S3) of the annual mean fire season wildfire burned areas. Variations of VPD
278 and precipitation not only affect fire season ignition likelihood and fire spread [*Holden*
279 *et al.*, 2018; *Sedano and Randerson*, 2014] through fuel moisture, but also regulate
280 vegetation growth, fuel structure [*Gale et al.*, 2021] (e.g., fuel composition and spatial
281 connectivity), and fuel availability [*Littell et al.*, 2009; *Littell et al.*, 2016; *Mueller et*
282 *al.*, 2020; *Van Der Werf et al.*, 2008]. The importance of these climate wetness variables
283 confirms the dominant roles of local water balances and air dryness for wildfire
284 prediction from sub-seasonal to seasonal scales [*Archibald et al.*, 2009; *Chen et al.*,
285 2011; *Littell et al.*, 2016] , especially in regions with large burned areas.

286 Furthermore, we found that the emergent functional relationships between climate
287 wetness and wildfire burned area were parabolic (Fig. S3): *i.e.*, enhancement of
288 historical precipitation or decline of historical VPD (indicating wetter conditions) first
289 increased burned area in more xeric conditions, then suppressed burned area under more
290 mesic conditions, consistent with previous findings in subtropical regions [*Andela and*
291 *Van Der Werf*, 2014; *Van Der Werf et al.*, 2008]. The transition points of these emergent
292 functional relationships (thresholds at which the relationships reverse) were region
293 specific, and these relationships may be useful for developing, tuning, and
294 benchmarking wildfire models [*Zhu et al.*, 2021].



295 For the time lags between those dominant climate wetness variables and fire-season
296 burned areas, our results demonstrated that burned area over NHAF was more
297 modulated by relatively short-term wetness (VPD during wet-to-dry and onset of dry
298 season, from September to December), while SHAF and SHSA burned areas depended
299 more on long-term wetness (precipitation during wet and wet-to-dry season, December
300 to March in SHAF, and November to April in SHSA) (Fig. 4g-i). The short-term
301 variations of climate wetness can directly affect near-surface temperature and moisture
302 availability, which affect fuel flammability [*Holden et al.*, 2018; *Littell et al.*, 2016],
303 while the long-term wetness (*e.g.*, during rainy season) can affect fuel availability,
304 composition, and spatial connectivity, which can result in even stronger long time-
305 lagged controls on dry-season burned areas [*Abatzoglou and Kolden*, 2013; *Andela and*
306 *Van Der Werf*, 2014; *Archibald et al.*, 2009; *Chen et al.*, 2011; *Littell et al.*, 2016; *Van*
307 *Der Werf et al.*, 2008].

308



309

310 **Fig. 4.** Spatial-temporal importance of climate wetness variables for burned area
 311 dynamics. (a-c) Spatial importance of climate wetness variables for fire-season burned
 312 areas. (d-f) statistical comparison of the climate wetness variable importance over
 313 regions with large and small burned areas. (g-i) fire season burned area dependency on
 314 the history of the climate wetness driver over Northern Hemisphere Africa (NHAF),
 315 Southern Hemisphere Africa (SHAF), and Southern Hemisphere South America
 316 (SHSA) regions.

317 Previous work has shown that when and where fires occurred during dry season
 318 can be affected by precipitation induced fuel availability patterns during wet and during
 319 wet-to-dry transition seasons in savannah ecosystems [Andela and Van Der Werf, 2014;
 320 Archibald et al., 2009; Van Der Werf et al., 2008]. Also, precipitation variations during
 321 wet and wet-to-dry transition seasons in the tropical forest ecosystem can affect soil
 322 recharge during wet season and further affect plant transpiration, local surface humidity,



323 and precipitation during the following dry season [*Chen et al.*, 2011; *Malhi et al.*, 2008;
324 *Ramos da Silva et al.*, 2008]. The exact responses of fires to short-and-long term climate
325 variations depend on both local wetness and fuel conditions (*e.g.*, fires in wetter
326 ecosystems with enough fuel availability can be mainly limited by the length of dry
327 season, while fires in drier ecosystems can be limited by fuel availability during wet
328 season [*Andela and Van Der Werf*, 2014; *Van Der Werf et al.*, 2008]). Therefore, an
329 effective way of integrating the climate wetness history (*i.e.*, AttentionFire model) can
330 lead to more accurate predictions of burned area spatial-temporal dynamics.

331 **3.3 Possible usage of oceanic index for long-leading time predictions**

332 In ASA regions, large-scale variations of oceanic dynamics can directly influence
333 local climate (*e.g.*, precipitation variations during wet seasons [*Andela and Van Der*
334 *Werf*, 2014; *Chen et al.*, 2011]) through time-lagged controls of teleconnections and
335 indirectly influence fires during following dry seasons [*Andela et al.*, 2017; *Chen et al.*,
336 2016; *Chen et al.*, 2011]. Therefore, we hypothesized that ocean dynamics might benefit
337 AttentionFire model predictions, especially for long leading time fire predictions
338 through providing additional information that has not been reflected in local climate
339 and land surface conditions [*Andela et al.*, 2017; *Chen et al.*, 2016; *Chen et al.*, 2020;
340 *Chen et al.*, 2011].

341 We compared model performance for short term (1-4 month ahead), and long term
342 (5-8 month ahead) fire predictions with and without considering the four oceanic
343 indexes. Relative to the MAE of short-term predictions, the mean MAE of long-term
344 predictions without and with teleconnections increased by ~34% and ~14% in NHAF,



~34% and ~15% in SHAF, and ~17% and ~7% in SHSA, respectively, indicating the decline of system predictability with longer leading time (Figure 5). However, for long-term predictions, including oceanic indexes and teleconnections could decrease the mean MAE by ~20%, ~19%, and ~11% in NHAF, SHAF, and SHSA regions, respectively, compared with the case without oceanic indexes. The results demonstrated the potential usage of teleconnections for longer than 5 months leading time burned area predictions.

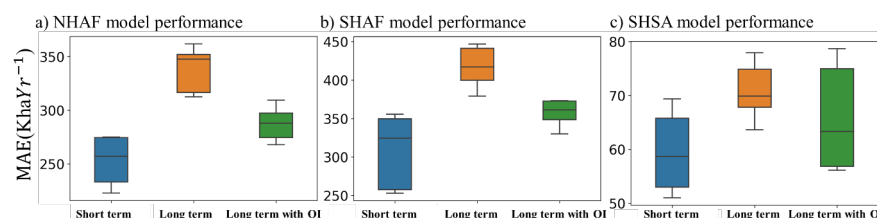


Fig. 5: Performance of AttentionFire burned area predictions with 1~4 month leading time (short-term) and with 5-8 month leading (long-term). MAE is mean absolute error. Long term prediction with OI means the AttentionFire model also considered four ocean indices that have been widely used for fire prediction over South American and African regions. Four OIs are: Oceanic Niño Index (ONI), Atlantic multidecadal Oscillation (AMO) index, Tropical Northern Atlantic (TNA) Index, and Tropical Southern Atlantic (TSA) Index.

3.4 Future trends of burned area over Africa and South America

Due to climate change and human activities [Andela *et al.*, 2017], strong but opposing trends of burned areas have been observed in Northern (decreasing) and Southern (increasing) Hemisphere Africa [Andela and Van Der Werf, 2014], and within different regions of Southern Hemisphere America [Andela *et al.*, 2017] during the



365 recent two decades, resulting in an overall declining burned area trend in Africa and
366 South America. However, whether this decline will persist is under debate. On one hand,
367 the projected increases in population, expansion of agriculture, mechanized (fire-free)
368 management, and fire suppression policies will likely continue to decrease burned areas
369 [*Andela and Van Der Werf*, 2014] (e.g., human activities were regarded as one of the
370 main drivers for fire decline in NHAF region). On the other hand, future climate change
371 [*Dai*, 2013; *Taufik et al.*, 2017] could outweigh human impacts and result in
372 unprecedented fire-prone environments in the tropics [*Malhi et al.*, 2008; *Pechony and*
373 *Shindell*, 2010] (e.g., fires showed strong dependency with climate wetness in NHAF,
374 SHAF [*Andela and Van Der Werf*, 2014; *Archibald et al.*, 2009] and SHSA [*Chen et al.*,
375 2011] regions).
376

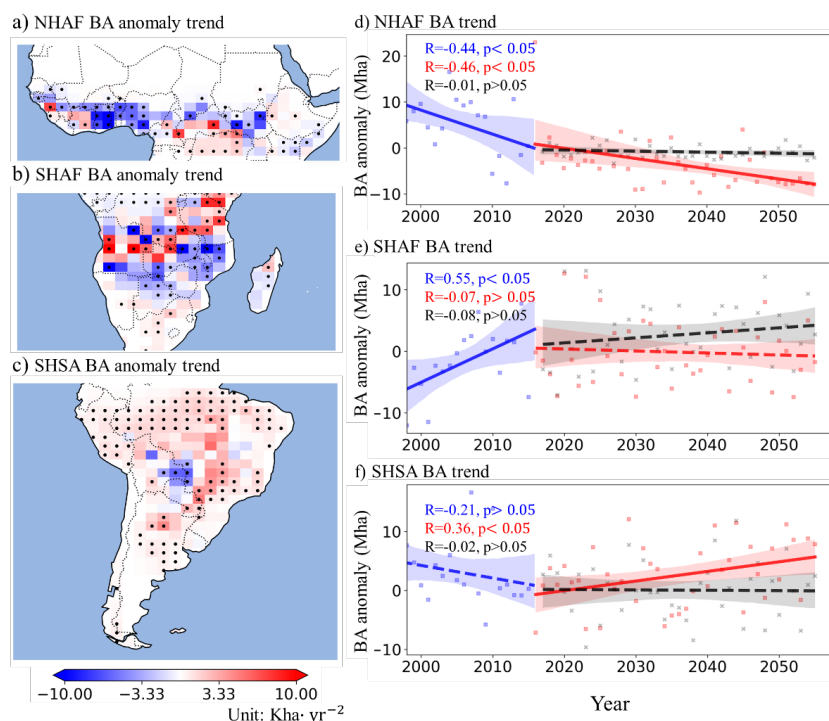


Fig. 6: Future burned area trends under the SSP585 high emission scenario. (a-c) spatial distribution of fire season burned area trends using drivers with interannual variations; dots in (a-c) indicate gridcells with statistically significant changes in the trend. (d-f) regionally aggregated burned area changes with historical mean subtracted. Blue and red lines respectively represent burned area anomaly in history and future; the black line represents future burned area trend while removing the interannual variations of the dominant variable. Solid lines represented significant BA trends (p value < 0.05) while dashed lines represented non-significant BA trends.

Considering land use changes, population growth, and projected climate under the SSP585 high emission scenario, our model predicted that burned areas in the NHAF region will continue to decline; the currently increasing trend will be dampened in the



389 SHAF region, and the currently decreasing trend will be reversed in SHSA region (Fig.
 390 6). Over NHAF and SHSA, burned area trends at the gridcell level are mostly robust
 391 (Fig. 6a-c; p value < 0.05) and of the same sign, thus resulting in a robust trend at
 392 regional scale.

393 To investigate what drives future burned area changes, we iteratively surrogated
 394 each driver with its climatology while keeping the other factors the same. Gridded
 395 burned area changing trends in NHAF and SHSA were mostly affected by VPD changes
 396 (Table S3), and removing VPD inter-annual changes resulted in non-significant burned
 397 area trends at the whole NHAF and SHSA region (Fig. 6). VPD was projected to
 398 continuously increase due to warming but had different implications over NHAF and
 399 SHSA. Over the relatively fuel abundant SHSA region, increased VPD will likely
 400 increase burned area (Pearson $r = 0.45$, p value < 0.05 , Fig. S4) through increasing fuel
 401 dryness and combustibility [Chen *et al.*, 2011; Kelley *et al.*, 2019; Malhi *et al.*, 2008;
 402 Van Der Werf *et al.*, 2008]. In contrast, over the semi-arid savannah dominated NHAF
 403 region (less fuel, compared with SHSA), higher VPD could decrease burned area
 404 (Pearson $r = -0.81$, p value < 0.05 , Fig. S4) through limiting plant growth and fuel
 405 availability [Andela *et al.*, 2017; Andela and Van Der Werf, 2014; Van Der Werf *et al.*,
 406 2008]. For the SHAF, population growth followed by climate changes (Table S3)
 407 showed stronger influences on grided burned area changes while the heterogeneity of
 408 wildfire responses finally led to a non-significant trend at the regional scale (Fig. 6).
 409 Our findings highlight the importance of climate changes on understanding future
 410 burned area dynamics, and motivate better representation of climate wetness effects on



411 wildfire dynamics in process-based and machine learning-based wildfire prediction
412 models.

413

414 **4. Conclusions**

415 This study developed an interpretable machine learning model (AttentionFire_v1.0)
416 for burned areas predictions over African and south American regions. Compared with
417 observations and other five widely used machine learning baseline models, we
418 demonstrated the effectiveness of the AttentionFire model to capture the magnitude,
419 spatial distribution, and temporal variation of burned areas. “Attention” mechanisms
420 enabled the interpretation of complex but critical spatial-temporal patterns [Guo *et al.*,
421 2019; Li *et al.*, 2020; Liang *et al.*, 2018; Qin *et al.*, 2017; Vaswani *et al.*, 2017], thus
422 uncovering the black-boxed relationships in machine learning models for burned area
423 predictions. We demonstrated the spatiotemporally heterogeneous and strong time-
424 lagged controls from local climate wetness on burned areas. Furthermore, under the
425 SSP585 high emission scenario, our results suggested that the increasing trend in
426 burned area over southern Africa will dampened, and the declining trend in burned area
427 over fuel abundant southern America will reverse. This study highlights the importance
428 of skillful representation of spatiotemporally heterogeneous and strong time-lagged
429 climate wetness effects on understanding wildfire dynamics and developing advanced
430 early fire warning models.

431

432 **Acknowledgements:**



433 This research was supported by the Director, Office of Science, Office of Biological
434 and Environmental Research of the US Department of Energy under contract no.
435 DEAC02-05CH11231 as part of their Regional and Global Climate Modeling program
436 through the Reducing Uncertainties in Biogeochemical Interactions through Synthesis
437 and Computation Scientific Focus Area (RUBISCO SFA) project and as part of the
438 Energy Exascale Earth System Model (E3SM) project.

439

440 **Code availability**

441 The source code of AttentionFire_v1.0 is archive at Zenodo repository:
442 <https://zenodo.org/record/6903284#.YuA3oOzMlaF>, under Creative Commons
443 Attribution 4.0 International license, with four zip files: data, data_preparation, model,
444 and example. The "data" file contains the links to all raw datasets used to drive the
445 model (e.g., burned areas, climate forcing). The "data_preparation" file contains the
446 code to preprocess the raw datasets and make them be ready for training and testing the
447 AttentionFire model. The "model" file contains the python code of AttentionFire model.
448 The "example" file gives a detailed example of how to use the AttentionFire model for
449 burned area predictions.

450 There is also a tutorial file "Data_Model_Tutorial" that contain descriptions on (1)
451 how to load the raw datasets; (2) how to prepare the input and output datasets for ML
452 model; (3) how to initialize the ML model and run the model (4) how to train the ML
453 model and use the trained ML model for predictions; (5) how to save and load the model
454 parameters and save the predicted results.



455

456 **Data availability**

457 **Burned area:** Global Fire Emissions Database

458 https://daac.ornl.gov/VEGETATION/guides/fire_emissions_v4.html

459 **NCEP-DOE Reanalysis Climate forcings:**

460 <https://psl.noaa.gov/data/gridded/data.ncep.reanalysis2.html>

461 **Population:** <https://landscan.ornl.gov/>

462 **Road density:** <https://www.globio.info/download-grip-dataset>

463 **Livestock density:** <https://www.fao.org/dad-is/en/>

464 **Land cover change:** <https://luh.umd.edu/data.shtml>

465 **Oceanic index:** <https://psl.noaa.gov/data/climateindices/list/>

466

467 **Author contributions**

468 QZ and FL designed the study. QZ, FL, and MC designed the model experiments. FL

469 wrote the code and ran the experiments. LZ, WR, JR, LX, HW, ZG, and JG all

470 contributed to the interpretation of the results and writing of the paper.

471

472 **References**

473 Abatzoglou, J. T., and C. A. Kolden (2013), Relationships between climate and macroscale area burned
 474 in the western United States, *International Journal of Wildland Fire*, 22(7), 1003-1020.

475 Amatulli, G., M. J. Rodrigues, M. Trombetti, and R. Lovreglio (2006), Assessing long-term fire risk at
 476 local scale by means of decision tree technique, *Journal of Geophysical Research: Biogeosciences*,
 477 111(G4).

478 Andela, N., D. C. Morton, L. Giglio, Y. Chen, G. Van Der Werf, P. S. Kasibhatla, R. DeFries, G. Collatz,
 479 S. Hantson, and S. Kloster (2017), A human-driven decline in global burned area, *Science*,
 480 356(6345), 1356-1362.



- Andela, N., and G. R. Van Der Werf (2014), Recent trends in African fires driven by cropland expansion and El Niño to La Niña transition, *Nature Climate Change*, 4(9), 791-795.
- Aragao, L. E. O., Y. Malhi, N. Barbier, A. Lima, Y. Shimabukuro, L. Anderson, and S. Saatchi (2008), Interactions between rainfall, deforestation and fires during recent years in the Brazilian Amazonia, *Philosophical Transactions of the Royal Society B: Biological Sciences*, 363(1498), 1779-1785.
- Archibald, S., D. P. Roy, B. W. van Wilgen, and R. J. Scholes (2009), What limits fire? An examination of drivers of burnt area in Southern Africa, *Global Change Biology*, 15(3), 613-630.
- Benavides-Solorio, J., and L. H. J. H. P. MacDonald (2001), Post-fire runoff and erosion from simulated rainfall on small plots, Colorado Front Range, 15(15), 2931-2952.
- Bowman, D. M., J. K. Balch, P. Artaxo, W. J. Bond, J. M. Carlson, M. A. Cochrane, C. M. D'Antonio, R. S. DeFries, J. C. Doyle, and S. P. Harrison (2009), Fire in the Earth system, *science*, 324(5926), 481-484.
- Chen, Y., D. C. Morton, N. Andela, L. Giglio, and J. T. Randerson (2016), How much global burned area can be forecast on seasonal time scales using sea surface temperatures?, *Environmental Research Letters*, 11(4), 045001.
- Chen, Y., J. T. Randerson, S. R. Coffield, E. Foufoula-Georgiou, P. Smyth, C. A. Graff, D. C. Morton, N. Andela, G. R. van der Werf, and L. Giglio (2020), Forecasting global fire emissions on subseasonal to seasonal (S2S) time scales, *Journal of advances in modeling earth systems*, 12(9), e2019MS001955.
- Chen, Y., J. T. Randerson, D. C. Morton, R. S. DeFries, G. J. Collatz, P. S. Kasibhatla, L. Giglio, Y. Jin, and M. E. Marlier (2011), Forecasting fire season severity in South America using sea surface temperature anomalies, *Science*, 334(6057), 787-791.
- Coffield, S. R., C. A. Graff, Y. Chen, P. Smyth, E. Foufoula-Georgiou, and J. T. Randerson (2019), Machine learning to predict final fire size at the time of ignition, *International journal of wildland fire*.
- Dai, A. (2013), Increasing drought under global warming in observations and models, *Nature climate change*, 3(1), 52-58.
- Etminan, M., G. Myhre, E. Highwood, and K. J. G. R. L. Shine (2016), Radiative forcing of carbon dioxide, methane, and nitrous oxide: A significant revision of the methane radiative forcing, 43(24), 12,614-612,623.
- Gale, M. G., G. J. Cary, A. I. Van Dijk, and M. Yebra (2021), Forest fire fuel through the lens of remote sensing: Review of approaches, challenges and future directions in the remote sensing of biotic determinants of fire behaviour, *Remote Sensing of Environment*, 255, 112282.
- Giglio, L., J. T. Randerson, and G. R. Van Der Werf (2013), Analysis of daily, monthly, and annual burned area using the fourth-generation global fire emissions database (GFED4), *Journal of Geophysical Research: Biogeosciences*, 118(1), 317-328.
- Gray, M. E., L. J. Zachmann, and B. G. Dickson (2018a), A weekly, continually updated dataset of the probability of large wildfires across western US forests and woodlands, *Earth System Science Data*, 10(3), 1715-1727.
- Gray, M. E., L. J. Zachmann, and B. G. J. E. S. S. D. Dickson (2018b), A weekly, continually updated dataset of the probability of large wildfires across western US forests and woodlands, 10(3), 1715-1727.
- Guo, T., T. Lin, and N. Antulov-Fantulin (2019), Exploring interpretable LSTM neural networks over multi-variable data, paper presented at International Conference on Machine Learning, PMLR.



- 525 Hantson, S., A. Arneth, S. P. Harrison, D. I. Kelley, I. C. Prentice, S. S. Rabin, S. Archibald, F. Mouillot,
 526 S. R. Arnold, and P. Artaxo (2016), The status and challenge of global fire modelling,
 527 *Biogeosciences*, 13(11), 3359-3375.
- 528 Hochreiter, S., and J. Schmidhuber (1997), Long short-term memory, *Neural computation*, 9(8), 1735-
 529 1780.
- 530 Holden, Z. A., A. Swanson, C. H. Luce, W. M. Jolly, M. Maneta, J. W. Oyler, D. A. Warren, R. Parsons,
 531 and D. Affleck (2018), Decreasing fire season precipitation increased recent western US forest
 532 wildfire activity, *Proceedings of the National Academy of Sciences*, 115(36), E8349-E8357.
- 533 Hurtt, G. C., L. Chini, R. Sahajpal, S. Frolking, B. L. Boudirsky, K. Calvin, J. C. Doelman, J. Fisk, S.
 534 Fujimori, and K. Klein Goldewijk (2020), Harmonization of global land use change and
 535 management for the period 850–2100 (LUH2) for CMIP6, *Geoscientific Model Development*,
 536 13(11), 5425-5464.
- 537 Jain, P., S. C. Coogan, S. G. Subramanian, M. Crowley, S. Taylor, and M. D. Flannigan (2020), A review
 538 of machine learning applications in wildfire science and management, *Environmental Reviews*,
 539 28(4), 478-505.
- 540 Joshi, J., and R. Sukumar (2021), Improving prediction and assessment of global fires using multilayer
 541 neural networks, *Scientific reports*, 11(1), 1-14.
- 542 Kelley, D. I., I. Bistinas, R. Whitley, C. Burton, T. R. Marthews, and N. Dong (2019), How contemporary
 543 bioclimatic and human controls change global fire regimes, *Nature Climate Change*, 9(9), 690-696.
- 544 Knorr, W., F. Dentener, J.-F. Lamarque, L. Jiang, and A. Arneth (2017), Wildfire air pollution hazard
 545 during the 21st century, *Atmospheric Chemistry and Physics*, 17(14), 9223-9236.
- 546 Lelieveld, J., J. S. Evans, M. Fnais, D. Giannadaki, and A. Pozzer (2015), The contribution of outdoor
 547 air pollution sources to premature mortality on a global scale, *Nature*, 525(7569), 367-371.
- 548 Leung, H., and S. Haykin (1991), The complex backpropagation algorithm, *IEEE Transactions on signal*
 549 *processing*, 39(9), 2101-2104.
- 550 Li, F., Z. Gui, Z. Zhang, D. Peng, S. Tian, K. Yuan, Y. Sun, H. Wu, J. Gong, and Y. Lei (2020), A
 551 hierarchical temporal attention-based LSTM encoder-decoder model for individual mobility
 552 prediction, *Neurocomputing*, 403, 153-166.
- 553 Liang, Y., S. Ke, J. Zhang, X. Yi, and Y. Zheng (2018), Geoman: Multi-level attention networks for geo-
 554 sensory time series prediction, paper presented at IJCAI.
- 555 Littell, J. S., D. McKenzie, D. L. Peterson, and A. L. Westerling (2009), Climate and wildfire area burned
 556 in western US ecoprovinces, 1916–2003, *Ecological Applications*, 19(4), 1003-1021.
- 557 Littell, J. S., D. L. Peterson, K. L. Riley, Y. Liu, and C. H. Luce (2016), A review of the relationships
 558 between drought and forest fire in the United States, *Global change biology*, 22(7), 2353-2369.
- 559 Malhi, Y., J. T. Roberts, R. A. Betts, T. J. Killeen, W. Li, and C. A. Nobre (2008), Climate change,
 560 deforestation, and the fate of the Amazon, *science*, 319(5860), 169-172.
- 561 Mueller, S. E., A. E. Thode, E. Q. Margolis, L. L. Yocom, J. D. Young, and J. M. Iniguez (2020), Climate
 562 relationships with increasing wildfire in the southwestern US from 1984 to 2015, *Forest Ecology*
 563 *and Management*, 460, 117861.
- 564 Pechony, O., and D. T. Shindell (2010), Driving forces of global wildfires over the past millennium and
 565 the forthcoming century, *Proceedings of the National Academy of Sciences*, 107(45), 19167-19170.
- 566 Qin, Y., D. Song, H. Chen, W. Cheng, G. Jiang, and G. Cottrell (2017), A dual-stage attention-based
 567 recurrent neural network for time series prediction, *arXiv preprint arXiv:1704.02971*.
- 568 Rabin, S. S., J. R. Melton, G. Lasslop, D. Bachelet, M. Forrest, S. Hantson, J. O. Kaplan, F. Li, S.



- Mangeon, and D. S. Ward (2017), The Fire Modeling Intercomparison Project (FireMIP), phase 1: experimental and analytical protocols with detailed model descriptions, *Geoscientific Model Development*, 10(3), 1175-1197.
- Ramanathan, V., P. Crutzen, J. Kiehl, and D. Rosenfeld (2001), Aerosols, climate, and the hydrological cycle, *science*, 294(5549), 2119-2124.
- Ramos da Silva, R., D. Werth, and R. Avissar (2008), Regional impacts of future land-cover changes on the Amazon basin wet-season climate, *Journal of climate*, 21(6), 1153-1170.
- Randerson, J. T., H. Liu, M. G. Flanner, S. D. Chambers, Y. Jin, P. G. Hess, G. Pfister, M. Mack, K. Treseder, and L. J. s. Welp (2006), The impact of boreal forest fire on climate warming, 314(5802), 1130-1132.
- Reichstein, M., G. Camps-Valls, B. Stevens, M. Jung, J. Denzler, and N. Carvalhais (2019), Deep learning and process understanding for data-driven Earth system science, *Nature*, 566(7743), 195-204.
- Sedano, F., and J. Randerson (2014), Multi-scale influence of vapor pressure deficit on fire ignition and spread in boreal forest ecosystems, *Biogeosciences*, 11(14), 3739-3755.
- Shvetsov, E. G., E. A. Kukavskaya, L. V. Buryak, and K. J. E. R. L. Barrett (2019), Assessment of post-fire vegetation recovery in Southern Siberia using remote sensing observations, 14(5), 055001.
- Taufik, M., P. J. Torfs, R. Uijlenhoet, P. D. Jones, D. Murdiyarso, and H. A. Van Lanen (2017), Amplification of wildfire area burnt by hydrological drought in the humid tropics, *Nature Climate Change*, 7(6), 428-431.
- Teckentrup, L., S. P. Harrison, S. Hantson, A. Heil, J. R. Melton, M. Forrest, F. Li, C. Yue, A. Arneth, and T. Hickler (2019), Response of simulated burned area to historical changes in environmental and anthropogenic factors: a comparison of seven fire models, *Biogeosciences*, 16(19), 3883-3910.
- Turco, M., S. Jerez, F. J. Doblas-Reyes, A. AghaKouchak, M. C. Llasat, and A. Provenzale (2018), Skilful forecasting of global fire activity using seasonal climate predictions, *Nature communications*, 9(1), 1-9.
- Van Der Werf, G. R., J. T. Randerson, L. Giglio, N. Gobron, and A. Dolman (2008), Climate controls on the variability of fires in the tropics and subtropics, *Global Biogeochemical Cycles*, 22(3).
- Vaswani, A., N. Shazeer, N. Parmar, J. Uszkoreit, L. Jones, A. N. Gomez, L. Kaiser, and I. Polosukhin (2017), Attention is all you need, *arXiv preprint arXiv:1706.03762*.
- Werf, G. R., J. T. Randerson, L. Giglio, T. T. v. Leeuwen, Y. Chen, B. M. Rogers, M. Mu, M. J. Van Marle, D. C. Morton, and G. J. J. E. S. S. D. Collatz (2017), Global fire emissions estimates during 1997–2016, 9(2), 697-720.
- Xu, X., G. Jia, X. Zhang, W. J. Riley, and Y. Xue (2020), Climate regime shift and forest loss amplify fire in Amazonian forests, *Global Change Biology*, 26(10), 5874-5885.
- Yu, Y., J. Mao, P. E. Thornton, M. Notaro, S. D. Wullschleger, X. Shi, F. M. Hoffman, and Y. Wang (2020), Quantifying the drivers and predictability of seasonal changes in African fire, *Nature communications*, 11(1), 1-8.
- Zhou, W., D. Yang, S.-P. Xie, and J. J. N. C. C. Ma (2020), Amplified Madden–Julian oscillation impacts in the Pacific–North America region, *Nature Climate Change*, 10(7), 654-660.
- Zhu, Q., F. Li, W. J. Riley, L. Xu, L. Zhao, K. Yuan, H. Wu, J. Gong, and J. T. Randerson (2021), Building a machine learning surrogate model for wildfire activities within a global earth system model, *Geoscientific Model Development Discussions*, 1-22.